DALTON

Synthesis, reactivity and structures of hafnium-containing homo- and hetero- (bi- and tri-) metallic alkoxides based on edge- and face-sharing bioctahedral alkoxometalate ligands†

Michael Veith,* Sanjay Mathur,* Charu Mathur and Volker Huch

Institute of Inorganic Chemistry, University of Saarland, PO 151150, D-66041, Saarbrücken, Germany

Using $[\{Hf(OPr^i)_4(Pr^iOH)\}_2]$ as a building-block precursor, a series of homo- and hetero-metallic alkoxides of hafnium has been prepared and characterised using elemental analyses, infrared, multinuclear (^{1}H, ^{7}Li, ^{13}C and ^{113}Cd) NMR and single-crystal X-ray diffraction studies. The solid-state structure of $[Hf_2(OPr^i)_8(Pr^iOH)_2]$ **1** reveals an edge-shared bioctahedral structure with the co-ordinated alcohol forming a hydrogen bridge across the dinuclear unit. The reactions of **1** with other nitrogen- or oxygen-containing donors gave monosubstituted products of the general formula $[Hf_2(OPr^i)_8(Pr^iOH)L]$ (L = C_5H_5N **2** or $C_4H_8O_2$ **3**) which retain the dinuclear edge-sharing bioctahedral structure as determined for **2** by X-ray crystallography. Compound **1** reacted (1:2) with $LiBu^n$ or $LiOPr^i$ to afford dimeric $[\{LiHf(OPr^i)_5\}_2]$ **4**. The molecular structure of **4** can be conceived as a dianionic $[Hf_2(OPr^i)_{10}]^{2-}$ unit that binds two Li^+ one on each side of the Hf–Hf vector which are additionally co-ordinated by the bridging OPr^i groups to display a trigonal-pyramidal geometry at the lithium atoms. The $Hf_2O_6Li_2$ core in **4** comprises two analogous seconorcubane subunits sharing a common face defined by a Hf_2O_2 ring. Equimolar reaction of $CuCl_2$ and $[KHf_2(OPr^i)_9]$ afforded the monomeric halide heterobimetallic derivative $[CuHf_2Cl(OPr^i)_9]$ **5**. Compound **5** is paramagnetic and follows Curie law behaviour as inferred by a variable-temperature ^{1}H NMR study. In the solid state its molecular geometry could be formally seen as a tetradentate interaction of the distorted confacial bioctahedron $[Hf_2(OPr^i)_9]^-$ with a $CuCl^+$ fragment. Each Hf is six-co-ordinated; Cu is five-co-ordinated and displays a distorted trigonal-bipyramidal geometry. The reaction (1:1) of $[CdHf_2I(OPr^i)_9]$ with $KSr(OPr^i)_3$ produced a new heterotermetallic derivative $[\{[Cd(OPr^i)_3]Sr[Hf_2(OPr^i)_9]\}_2]$ **6**. This involves the switching of central metal atoms between the two precursors and the $Hf_2(OPr^i)_9$ unit in **6** binds to Sr rather than Cd as anticipated. The centrosymmetric dimeric form of **6** is made up of a $[Sr(\mu\text{-}OPr^i)_2Cd(\mu\text{-}OPr^i)_2Cd(\mu\text{-}OPr^i)_2Sr]^{2+}$ spirocyclic unit capped at both the ends by $[Hf_2(OPr^i)_9]^-$ moieties.

There is continuing interest in heterometal alkoxides, in part, because large heterometal assemblies (metal–metal bonded or anion-bridged metal centres) can provide access to molecular-based systems displaying properties which may find applications in molecular electronics or optical switching devices.[1] Among the tetravalent early transition metals the alkoxide chemistry of titanium and zirconium is most studied as shown by their frequent use as heterometal partners to a large number of metals throughout the Periodic Table.[2] However, in contrast to titanium and zirconium, well characterised examples of hafnium are scarce, despite the fact that hafnium-containing ceramics, in view of their large relative permittivities, are finding increasing applications in the reliable production of ultra-large-scale integration (ULSI) memory devices.[3]

In earlier studies[4] the isopropoxides of some of the tetravalent metals (Sn, Zr, Hf and Ce) were suggested to be dimeric alcoholates of general formula $[M_2(OPr^i)_8(Pr^iOH)_2]$ with an edge-sharing bioctahedral structure. This was later verified for Sn,[5] Zr[6] and Ce[6] by solid-state structural studies which additionally showed a *trans* positioning (across the M–M vector) of neutral (ROH) ligands and the existence of hydrogen bonding [R(M)O···H···OR]. In view of the increasing applications of hafnium-containing ceramics[7] and the dearth of data on synthetic and structural aspects of hafnium alkoxides, we initiated the present investigations on the synthesis, structure and reactivity of homo- and hetero-metal hafnium alkoxide derivatives.

† *Non-SI unit employed*: Torr ≈ 133 Pa.

Results and Discussion

Syntheses and spectroscopic characterisation

Owing to the presence of two neutral ligands, $[Hf_2(OPr^i)_8(Pr^iOH)_2]$ **1** is an interesting synthon since these ligands can be replaced with other donor molecules and in the absence of a donor ligand the co-ordinative unsaturation is expected to result in a structural change. Unless drastic conditions for expulsion are used, the co-ordinated alcohol in $[M_2(OPr^i)_8(Pr^iOH)_2]$ derivatives shows a tendency for retention and samples of $[Hf_2(OPr^i)_8(Pr^iOH)_2]$ heated in vacuum (30 min, 100 °C, 10^{-2} Torr), when recrystallised from mixtures of toluene–pyridine and –1,4-dioxane, produced $[Hf_2(OPr^i)_8(Pr^iOH)(NC_5H_5)]$ **2** and $[Hf_2(OPr^i)_8(Pr^iOH)(O_2C_4H_8)]$ **3**, respectively (Scheme 1). However authentic samples of alcohol-free hafnium isopropoxide $[Hf(OPr^i)_4]_n$, as indicated by the analytical data and absence of OH stretching frequencies in the IR spectra, could be obtained on prolonged (>4 h) pumping of hafnium isopropoxide at higher temperatures (140 °C, 10^{-2} Torr). Besides the characteristic stretching frequencies of metal-attached isopropoxy groups,[4] the IR spectra (KBr and $CDCl_3$) of **2** and **3** show broad OH stretching bands (see Experimental section) indicative of the hydrogen bonding present in both solution and solid state. The room-temperature ^{1}H and ^{13}C NMR spectra of **2** and **3** exhibit a single time-averaged environment for isopropyl groups suggesting a rapid exchange among different (bridging, terminal and neutral) types of ligands present in the molecule. As indicated by elemental analyses, cryoscopic and spectral studies, the formulation of **2** and **3** as $[Hf_2(OPr^i)_8(Pr^iOH)L]$

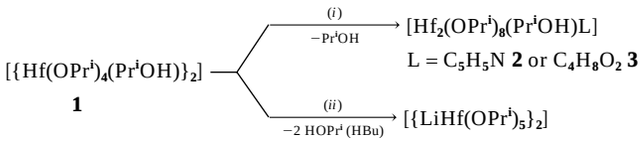

Scheme 1 (*i*) L; (*ii*) 2 LiOPr^i (LiBu^n)

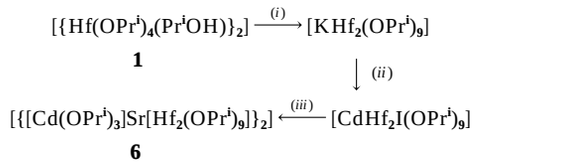

Scheme 2 (*i*) KOPr^i; (*ii*) CdI$_2$; (*iii*) KSr(OPr^i)$_3$

(L = C_5H_5N **2** or $C_4H_8O_2$ **3**) was supported by the single-crystal X-ray study performed on **2**. Various attempts at an X-ray crystallographic analysis of compound **3** were not successful.

In the light of the solid-state structure of compound **1** (see below), the edge-sharing octahedral framework can be viewed as a dianionic $[Hf_2(OPr^i)_{10}]^{2-}$ moiety which binds two H^+ in a bidentate fashion. In order to replace this electrophile (H^+) by any other monovalent cation the reaction of **1** was performed with LiBu^n or LiOPr^i to obtain dimeric [{LiHf(OPr^i)$_5$}$_2$] **4** (Scheme 1). In contrast to **1**–**3**, compound **4** is stereochemically rigid and the ambient-temperature ^{1}H NMR spectrum exhibits three overlapping doublets which could be resolved at −10 °C as three sets of signals in 2:2:1 intensity ratio, which is consistent with the solid-state structure of **4** showing three types of alkoxide ligands (Hf–OPr^i, Hf–μ-OPr^i, Hf–μ_3-OPr^i–Li) and is also corroborated by ^{13}C NMR spectral data (see Experimental section). The ^{7}Li NMR spectrum in [$^2H_8$]toluene shows a sharp resonance at δ 3.02. Molecular-weight studies performed in freezing benzene support the dimeric tendency (molecular complexity, η = 1.9) of **4**.

To explore the ligating behaviour of hafnium-based dinuclear alkoxometalate moieties toward bivalent cations, an anion-exchange reaction was performed in benzene between anhydrous $CuCl_2$ and [$KHf_2(OPr^i)_9$].[8a] The reaction mixture, after work-up, afforded a green solid in high yield (>90%) which could be crystallised from cold (0 °C) pentane as transparent green crystals of varying morphologies. The elemental analyses conform to the formulation [$CuHf_2Cl(OPr^i)_9$] **5**. The presence of Cu^{II} imparts paramagnetic behaviour to **5** and the room-temperature ^{1}H and ^{13}C NMR spectra are not structurally diagnostic. The ambient-temperature ^{1}H NMR spectrum however indicates a non-fluxional molecule with *gem*-dimethyl protons appearing as three broad doublets (δ 0.92, 1.35 and 1.44); the methine protons are observed as two broad overlapping multiplets (δ 4.27 and 4.70). Given the paramagnetism of **5** variable-temperature NMR studies were performed and the chemical shifts show a linear relationship with T^{-1} which is in agreement with a simple Curie law. At 40 °C the methyl signal appears as two resonances which integrate approximately 4:5; the latter signal being sharper presumably corresponds to OPr^i groups experiencing less paramagnetic influence away from the copper centre (see below). A similar behaviour observed for the titanium analogue [$CuTi_2Cl(OPr^i)_9$][8b] has been detailed elsewhere.

The heavy alkaline-earth elements are important constituents of a wide range of solid-state materials with diverse electronic and chemical properties including the high T_c superconductors (*e.g.* $YBa_2Cu_3O_{7-\delta}$,[9] $Bi_2Sr_2CaCu_2O_8$[10]) and pervoskite-based methane oxidation catalysts[11] (*e.g.* MM′O_3: M = Ca, Sr or Ba; M′ = Ti, Zr, Hf or Ce). The controllable and easy incorporation of alkaline-earth metals in heterometallic systems is a challenge that is posed by the interplay of materials science and metal alkoxide chemistry. In analogy to KBa(OPr^i)$_3$,[12] used as a novel anion, [$Ba(OPr^i)_3$]$^-$, transfer reagent with halide heterobimetallic precursors [$CdM_2I(OPr^i)_9$] (M = Ti,[8a] Zr[12] or Hf[8a]) for the facile and stoichiometrically precise incorporation of Ba^{2+} in heteropolymetallic alkoxide assemblies [{[Cd(OPr^i)$_3$]Ba[M$_2$(OPr^i)$_9$]}$_2$],[8a,12] the strategy was examined for the incorporation of strontium which assumes significance since the alkoxides of heavy alkaline-earth metals are essential (owing to the size effect) constituents of conducting multimetallic ceramics, *e.g.* $La_{2-x}Sr_2CuO_4$[13] and $Bi_2Sr_2CaCu_2O_8$.[10]

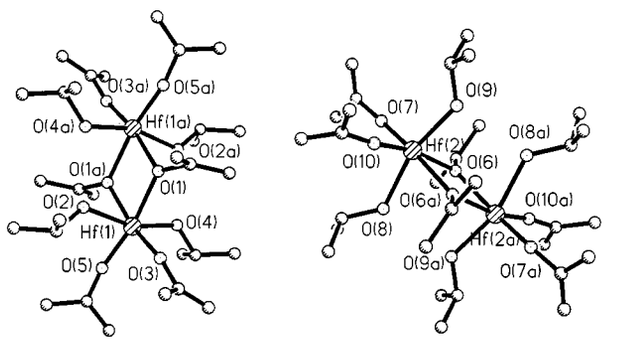

Fig. 1 Two crystallographically independent molecules in the unit cell of [{Hf(OPr^i)$_4$(Pr^{i}OH)}$_2$] **1**. Hydrogen atoms of the isopropyl groups are omitted for clarity. Atoms designated with an 'a' are related by symmetry. The 'bending' of axial ligands (across the Hf–Hf vector) is indicative of the hydrogen bridges present between O(2) and O(4a) [O(4) and O(2a)] not shown

An equimolar reaction of the recently reported [$CdHf_2I(OPr^i)_9$][8a] with freshly synthesized [{$KSr(OPr^i)_3$}$_n$] in toluene afforded [{[Cd(OPr^i)$_3$]Sr[Hf$_2$(OPr^i)$_9$]}$_2$] **6** in almost quantitative yield (Scheme 2). The molecule **6** is stereochemically rigid and the room-temperature spectra (^{1}H, ^{13}C and ^{113}Cd) are indicative of the structural pattern existing in solution. The ^{1}H NMR spectrum exhibits six methyl signals in an intensity ratio 4:2:8:4:4:2 whereas the methine protons are observed as three overlapping septets that integrate 10:6:8. The ^{13}C NMR spectrum displays five and six signals for the methine and methyl carbons in intensity ratios 8:2:4:4:6 and 6:4:4:4:2:4, respectively. The ^{113}Cd NMR chemical shift (δ 226.91) is comparable with the solution- and solid-state ^{113}Cd NMR chemical shifts observed for four-co-ordinate cadmium in [{[Cd(OPr^i)$_3$]Ba[M$_2$(OPr^i)$_9$]}$_2$] (M = Ti, Zr or Hf)[8a,12] derivatives. This along with the cryoscopic data supports the retention of the heterotermetallic nature and dimeric form of **6**, as observed in the solid state (see below), in solution too.

Solid-state and molecular structures

Five hafnium isopropoxide derivatives have been characterised by single-crystal X-ray diffraction studies during this work. A summary of the data collection and crystallographic parameters are given in Table 8.

[{Hf(OPr^i)$_4$(Pr^{i}OH)}$_2$] 1. Single crystals of compound **1** suitable for an X-ray diffraction study were grown from a cold (+10 °C) isopropyl alcohol solution and are made up of discrete dimers of Hf(OPr^i)$_4$·Pr^{i}OH molecules (Fig. 1). Compound **1** crystallises‡ in the triclinic space group *P*1 and the unit cell contains two crystallographically independent but structurally similar molecules of point group C_i (Fig. 1). Selected interatomic distances and angles for compound **1** are listed in Table 1. The central metal–oxygen unit is a planar rhombic Hf–O–Hf–O oxametallacycle lying on crystallographic inversion centres. Within the dimeric Hf_2O_{10} unit, both the Hf atoms bonded to three terminal OPr^i, two bridging OPr^i and one terminal Pr^{i}OH ligand show similar geometries, derived from a regular octahedron. The μ-OPr^i ligands are situated nearly symmetrically between the two Hf atoms [Hf(1)–O(1) 2.148(6);

‡ The unit-cell constants given in ref. 6 do not match ours.

Table 1 Selected bond lengths (Å) and angles (°) of compound **1**

Molecule **A**		Molecule **B**	
Hf(1)–O(5)	1.932(8)	Hf(2)–O(7)	1.944(7)
Hf(1)–O(4)	2.143(7)	Hf(2)–O(6a)	2.155(5)
Hf(1)–O(3)	1.938(8)	Hf(2)–O(8)	2.243(7)
Hf(1)–O(2)	2.185(7)	Hf(2)–O(9)	2.082(7)
Hf(1)–O(1)	2.148(6)	Hf(2)–O(10)	1.911(8)
Hf(1)–O(1a)	2.160(6)	Hf(2)–O(6)	2.156(6)
O(5)–Hf(1)–O(3)	97.5(4)	O(10)–Hf(2)–O(9)	99.6(3)
O(3)–Hf(1)–O(4)	97.3(3)	O(10)–Hf(2)–O(9)	95.3(3)
O(3)–Hf(1)–O(1)	95.1(3)	O(9)–Hf(2)–O(6a)	86.5(3)
O(5)–Hf(1)–O(1a)	94.4(3)	O(7)–Hf(2)–O(6a)	94.2(3)
O(4)–Hf(1)–O(1a)	83.3(3)	O(6a)–Hf(2)–O(6)	72.9(2)
O(5)–Hf(1)–O(2)	94.4(3)	O(7)–Hf(2)–O(6)	91.9(3)
O(4)–Hf(1)–O(2)	161.6(3)	O(6a)–Hf(2)–O(8)	79.1(2)
O(1a)–Hf(1)–O(2)	81.8(3)	O(10)–Hf(2)–O(8)	96.7(4)
O(5)–Hf(1)–O(4)	97.4(4)	O(7)–Hf(2)–O(9)	99.9(3)
O(5)–Hf(1)–O(1)	167.3(3)	O(7)–Hf(2)–O(6a)	165.3(3)
O(4)–Hf(1)–O(1)	83.1(3)	O(10)–Hf(2)–O(6)	166.8(3)
O(3)–Hf(1)–O(1a)	167.9(3)	O(9)–Hf(2)–O(6)	85.6(3)
O(1)–Hf(1)–O(1a)	73.0(3)	O(10)–Hf(2)–O(8)	92.1(3)
O(3)–Hf(1)–O(2)	95.1(3)	O(9)–Hf(2)–O(8)	162.2(3)
O(1)–Hf(1)–O(2)	82.4(3)	O(6)–Hf(2)–O(8)	80.2(2)
Hf(1)–O(1)–Hf(1a)	107.0(3)	Hf(2a)–O(6)–Hf(2)	107.1(2)

Hf(1)–O(1a) 2.160(6) Å]; the oxygen atoms of bridging OPr^i groups are planar (sum of angles = 359.9°) and have longer Hf–O contacts in comparison to the terminal Hf–O (1.93 Å) distances.

The overall molecular structure, as observed for the analogous $[M_2(OPr^i)_8(Pr^iOH)_2]$ (M = Sn, Zr or Ce) derivatives,[5,6] is a distorted edge-sharing bioctahedron comprising a '$(RO)_2Hf(\mu\text{-}OR)Hf(OR)_2$' plane with *trans* alcohol ligands (axial) on each hafnium atom. It is noteworthy that the two molecules (**A** and **B**) present in the unit cell differ remarkably in Hf–O distances of the axial ROH and RO^- ligands [(molecule **A**: Hf(1)–O(2) 2.185, Hf(1)–O(4) 2.143 Å; molecule **B**: Hf(2)–O(8) 2.243, Hf(2)–O(9) 2.082 Å] whereas the Hf–O distances in the $(RO)_2Hf(\mu\text{-}OR)Hf(OR)_2$ plane are comparable (Table 1). However, the axial Hf–O bond lengths in both molecules are sufficiently different to distinguish between alkoxide (average 2.112 Å) and alcohol ligands (average 2.214 Å). Hydroxylic hydrogen atoms of the neutral (ROH) ligands could not be located crystallographically, however their presence can be inferred from the ^{1}H NMR and Fourier-transform IR data. The distortion of Hf(1)–O(2) and Hf(1)–O(4) from regular octahedral geometry is consistent with the presence of a hydrogen bridge in the dimeric unit of **1**. Despite the long non-bonded Hf · · · Hf separation [3.463 (molecule **A**) and 3.468 Å (**B**)], the axial OR and ROH ligands are considerably bent (O · · · O 2.78 Å) toward each other. The average Hf–Hf(a)–OPr^i and Hf–Hf(a)–O(H)Pr^i angles (Table 2), 83.3 and 78.8° respectively, indicate the asymmetric nature of the hydrogen bonding and also that the weakly bound (ROH) ligands bend more; the bending of axial ligands in $[M_2(OPr^i)_8(Pr^iOH)_2]$ (M = Sn, Zr, Hf or Ce) derivatives seems to be *prima facie* evidence for hydrogen bonding since no such bending of ligands is observed in the structure of $Nb_2(OMe)_{10}$[14a] and $Nb_2(OPr^i)_{10}$[14b] which do not contain neutral ROH ligands. The exocyclic Hf–O–C angles are nearly linear (average 167.4°) corroborating a strong O→M π donation.[15]

The significant features of an edge-sharing bioctahedral unit present in $[M_2(OPr^i)_8(Pr^iOH)_2]$ (M = Sn, Zr, Hf or Ce) derivatives are summarised in Table 2. There appears to be no significant correlation between the M · · · M and O · · · O distances with increasing metal(IV) size. However in view of the variation of O–M–M (81.1–85.3°) and HO–M–M (80.9–71.4°) angles it is conceivable that with increasing M · · · M non-bonding separation the weakly co-ordinated ROH ligand shows an increased bending required for an effective hydrogen bonding since the O · · · O distances do not alter much (Table 2).

Table 2 Typical interatomic distances (Å) and angles (°) found in the solid-state structures of $[M_2(OPr^i)_8(Pr^iOH)_2]$ (M = Sn,[5] Zr,[6] Hf or Ce[6]) derivatives

M^{IV} (r/Å)	O · · · O in axial ligands	M · · · M vector	O–M–M	HO–M–M
Sn (0.71)	2.703	3.361	81.1	80.9
Zr (0.80)	2.770	3.490	85.3	75,9
Hf (0.86)*	2.789	3.465	83.3	78.8
Ce (0.92)	2.748	3.770	83.9	71.4

* Average values for molecules **A** and **B**.

Table 3 Selected bond lengths (Å) and angles (°) of compound **2**

Hf–O(4)	1.929(6)	Hf–O(2)	1.944(7)
Hf–O(1a)	2.175(5)	Hf–O(3)	2.154(6)
Hf–O(1)	2.178(5)	Hf–N	2.30(2)
Hf–O(5)	2.10(2)		
O(4)–Hf–O(2)	99.3(3)	O(4)–Hf–O(5)	88.6(4)
O(2)–Hf–O(5)	91.5(5)	O(4)–Hf–O(3)	90.7(3)
O(2)–Hf–O(3)	92.7(2)	O(5)–Hf–O(3)	175.8(5)
O(4)–Hf–O(1a)	165.8(3)	O(2)–Hf–O(1a)	94.6(3)
O(5)–Hf–O(1a)	94.2(4)	O(3)–Hf–O(1a)	85.5(2)
O(4)–Hf–O(1)	96.2(3)	O(2)–Hf–O(1)	164.5(3)
O(5)–Hf–O(1)	89.7(5)	O(3)–Hf–O(1)	86.2(2)
O(1a)–Hf–O(1)	69.9(2)	O(4)–Hf–N	96.0(5)
O(2)–Hf–N	92.1(5)	O(3)–Hf–N	171.0(5)
O(1a)–Hf–N	86.6(5)	O(1)–Hf–N	87.1(5)
Hf(a)–O(1)–Hf	108.6(2)		

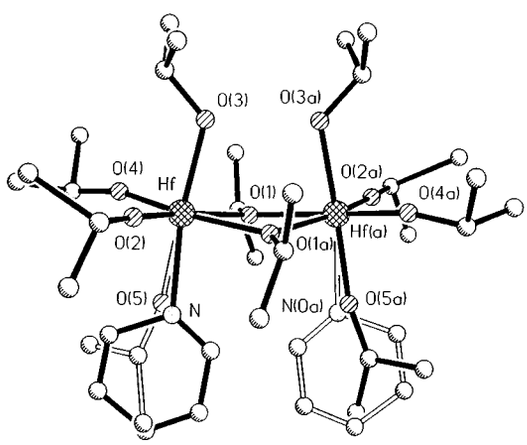

Fig. 2 Ball-and-stick view of $[Hf_2(OPr^i)_8(Pr^iOH)(NC_5H_5)]$ **2** with selected atom numbering. The lighter lines show the superposition of molecules. Hydrogen atoms are omitted for clarity

$[Hf_2(OPr^i)_8(Pr^iOH)(NC_5H_5)]$ 2. Crystals of compound **2** were grown from a toluene–pyridine solution at room temperature. The X-ray structural analysis confirmed the dimeric nature of this compound and a ball-and-stick view of the solid-state structure is shown in Fig. 2. Selected bond lengths and angles are summarised in Table 3. The centrosymmetry of the Hf_2O_2 core is not retained upon the reaction of the parent compound **1** with pyridine, as the stereoselective substitution of only one of the Pr^iOH ligands by pyridine takes place. The configuration is similar to that of **1**, *viz*. edge-sharing bioctahedral with the geometry around the hafnium atom being constituted by one neutral (Pr^iOH/pyridine) and three exo- and two endo-cyclic anionic (OR^-) ligands. In the solid state the molecules of **2** are stacked in a disordered manner and their superposition as shown in Fig. 2 does not allow a rigorous discussion of bond lengths and angles. However, the presence of hydrogen bonding *trans* to the disordered pyridine ligand is evident in the significant bending of the Hf–O(3) and Hf–O(3a) bonds.

Table 4 Selected bond lengths (Å) and angles (°) of compound **4**

Hf(1)–O(4)	1.938(8)	Hf(1)–O(5)	1.936(9)
Hf(1)–O(3)	2.065(9)	Hf(1)–O(2)	2.081(8)
Hf(1)–O(1)	2.226(8)	Hf(1)–O(1^{I})	2.232(7)
O(1)–Hf(1^{I})	2.232(7)	O(1)–Li^{II}	2.06(3)
O(2)–Li^{III}	1.85(3)	Li–O(2^{III})	1.85(3)
O(3)–Li^{II}	1.86(3)	Li–O(1^{IV})	2.06(3)
Li–O(3^{IV})	1.86(3)		
O(4)–Hf(1)–O(5)	100.5(5)	O(4)–Hf(1)–O(3)	95.2(4)
O(5)–Hf(1)–O(3)	92.9(4)	O(4)–Hf(1)–O(2)	93.5(4)
O(5)–Hf(1)–O(2)	94.4(4)	O(3)–Hf(1)–O(2)	167.5(3)
O(4)–Hf(1)–O(1)	96.7(3)	O(5)–Hf(1)–O(1)	162.4(4)
O(3)–Hf(1)–O(1)	81.8(3)	O(2)–Hf(1)–O(1)	88.2(3)
O(4)–Hf(1)–O(1^{I})	160.7(4)	O(5)–Hf(1)–O(1^{I})	98.3(4)
O(3)–Hf(1)–O(1^{I})	87.9(3)	O(2)–Hf(1)–O(1^{I})	81.0(3)
O(1)–Hf(1)–O(1^{I})	64.9(3)	Li^{II}–O(1)–Hf(1)	87.8(9)
Hf(1)–O(1)–Hf(1^{I})	115.1(3)	Li^{II}–O(1)–Hf(1^{I})	88.3(9)
Li^{II}–O(3)–Hf(1)	98.5(10)	Li^{III}–O(2)–Hf(1)	98.9(10)
O(2^{III})–Li–O(3^{IV})	126(2)	O(2^{III})–Li–O(1^{IV})	91.2(12)
O(3^{IV})–Li–O(1^{IV})	91.4(12)		

Symmetry transformations used to generate equivalent atoms: I $-x$, $-y$, $-z+1$; II $x-1$, y, z; III $-x+1$, $-y$, $-z+1$; IV $x+1$, y, z.

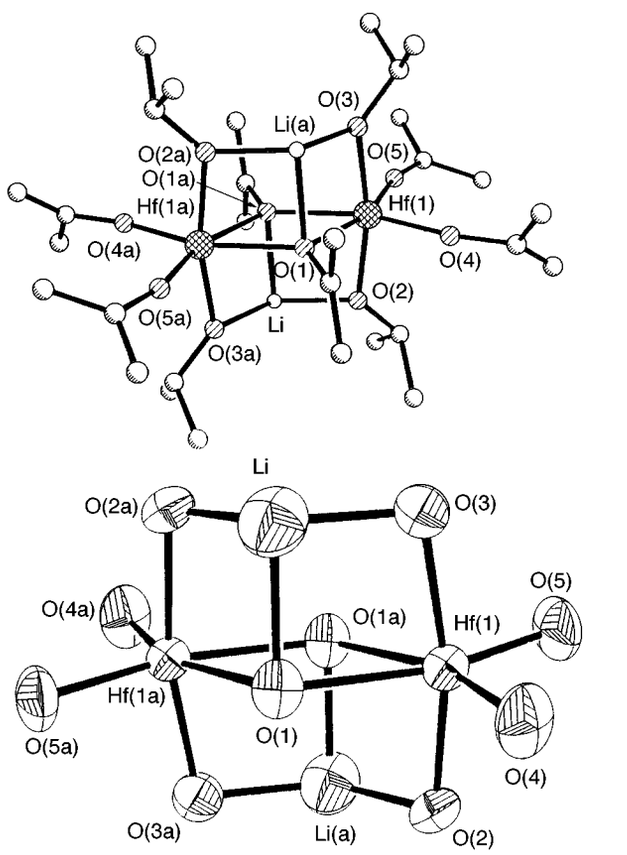

Fig. 3 Ball-and-stick drawing of the dimeric [{LiHf(OPr^{i})$_5$}$_2$] **4**, omitting the hydrogen atoms and an ORTEP plot of the metal–oxygen core. Atoms designated with an 'a' are generated by symmetry operations I–IV given in Table 4

[{LiHf(OPr^{i})$_5$}$_2$] 4. The compound of empirical formula LiHf(OPr^{i})$_5$ is dimeric in the solid state and possesses crystallographic C_i point symmetry. A ball-and-stick drawing of the molecular structure of **4** with the atom numbering scheme and an ORTEP[16] plot emphasising the metal–oxygen core are shown in Fig. 3. The salient bond lengths and angles are summarised in Table 4. The overall molecular architecture is reminiscent of the solid-state structure of [Hf_2(OPr^{i})$_8$(Pr^{i}OH)$_2$] **1** where the hydrogen atoms of the two *trans* Pr^{i}OH ligands have been replaced by lithium atoms, but which are additionally co-ordinated by the bridging isopropoxo groups. The two hafnium centres [Hf(1) and Hf(1a)] display a distorted-octahedral arrangement of ligands whereas the lithium atoms are located on the apices of the two distorted trigonal pyramids. The metal–oxygen core can be viewed as two analogous seconorcubane subunits sharing a common face, defined by the four-membered Hf_2O_2 ring. The central unit resembles the known structures of [{MSn(OBu^{t})$_3$}$_2$] (M = Li or Na)[17] and [{LiTi(OPr^{i})$_5$}$_2$],[18] however, in contrast to the four-co-ordinated lithium atoms in [{LiSn(OBu^{t})$_3$}$_2$] and [{LiTi(OPr^{i})$_5$}$_2$], the lithium centres in **4** are three-co-ordinated. Despite the similarity in formulation and nature of the heterometal partners, the co-ordination geometries of the metal atoms in **4** are entirely different from that observed in [{LiTi(OPr^{i})$_5$}$_2$]; Li and Hf are three- and six-co-ordinate in **4** in comparison to the four- and five-co-ordinate environments of Li and Ti in the latter case. This change in the ligand geometries is attributable to the pronounced tendency of larger tetravalent metals (Zr, Hf, Ce) to achieve six-co-ordination. Thus in **4** the co-ordination of O(1) and O(1a) to Li and Li(a), respectively, is sacrificed and the two oxygen atoms instead bind to the larger hafnium centres. Each hafnium possesses two terminal, two bridging (μ) and two triply bridging (μ_3) isopropoxide ligands. Bond lengths from Hf to OPr^{i} increase in the order Hf–O (terminal) [1.935(8)–1.936(9) Å] < Hf–μ-OLi [2.065(9)–2.081(8) Å] < Hf–μ_3-O [2.226(8)–2.232(7) Å]. The distortion in the octahedral environment of Hf is seen in the opening of the O(4)–Hf–O(5) angle [100.5(5)°] and narrowing of the O(3)–Hf(1)–O(2) angle [167.5(3)°] and is probably a combined effect of the steric demands of the isopropxy groups and the geometric constraints of the co-ordination environment about lithium. Lithium is bound by two bridging OPr^{i} groups in a symmetrical fashion [Li–O(3^{IV}) 1.86(3) and Li–O(2^{III}) 1.85(3) Å]; the Li–μ_3-O distance is 2.06(3) Å. Lithium although three-co-ordinate shows no significant C···Li contacts (shortest 2.932 Å) or any interaction in the typical range (1.85–2.40 Å) of agostic interactions. The Hf–O(terminal)–C angles (167.2–169.0°) approach linearity.

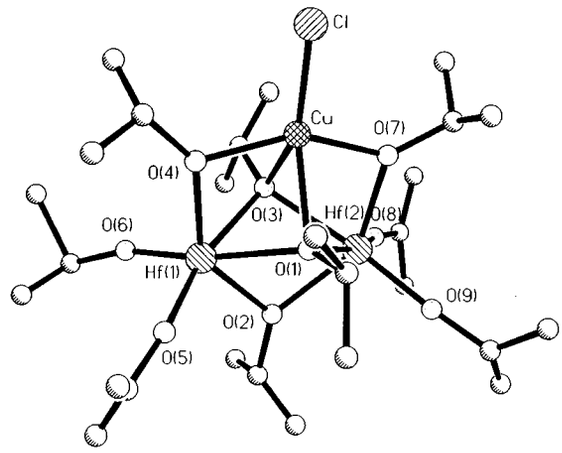

Fig. 4 Ball-and-stick representation of the solid-state structure of [$CuHf_2Cl$(OPr^{i})$_9$] **5** with the atom labelling scheme. Hydrogen atoms have been omitted for clarity

[$CuHf_2Cl$(OPr^{i})$_9$] 5. Compound **5** crystallises as a monomer in the monoclinic space group $P2_1/n$. A ball-and-stick view of the solid-state structure is shown in Fig. 4 and pertinent bond distances and angles are given in Table 5. The molecule belongs to the class of halide heterobimetallic derivatives [CdM_2I(OPr^{i})$_9$] (M = Sn,[19] Ti,[8a] Zr[12] or Hf[8a]) and [CuM_2Cl(OPr^{i})$_9$] (M = Ti[8b] or Zr[20]) where the bivalent central metal atom is co-ordinated by the M_2(OPr^{i})$_9^-$ confacial bioctahedral unit in a tetradentate manner. The heterometallic framework ($CuHf_2$) of compound **5** forms an isosceles triangle (non-bonded Hf···Cu and Hf···Hf distances being 3.303 and 3.259 Å, respectively) held together by three doubly (μ) bridging [O(2), O(4) and O(7)] and two triply (μ_3) bridging isopropoxo groups [O(1) and O(3)].

Table 5 Pertinent bond lengths (Å) and angles (°) of compound **5**

Hf(1)–O(6)	1.926(11)	Hf(1)–O(5)	1.932(10)
Hf(1)–O(4)	2.074(9)	Hf(1)–O(2)	2.181(8)
Hf(1)–O(1)	2.211(8)	Hf(1)–O(3)	2.233(8)
Hf(2)–O(8)	1.921(10)	Hf(2)–O(9)	1.931(10)
Hf(2)–O(7)	2.081(10)	Hf(2)–O(2)	2.143(9)
Hf(2)–O(1)	2.210(8)	Hf(2)–O(3)	2.221(8)
Cu–O(4)	2.001(10)	Cu–O(7)	2.008(10)
Cu–Cl	2.144(5)	Cu–O(1)	2.183(9)
Cu–O(3)	2.187(9)		
O(6)–Hf(1)–O(5)	99.4(5)	O(6)–Hf(1)–O(4)	101.8(5)
O(5)–Hf(1)–O(4)	106.6(4)	O(6)–Hf(1)–O(2)	102.3(4)
O(5)–Hf(1)–O(2)	100.9(4)	O(4)–Hf(1)–O(2)	139.6(4)
O(6)–Hf(1)–O(1)	164.0(4)	O(5)–Hf(1)–O(1)	96.1(4)
O(4)–Hf(1)–O(1)	76.9(3)	O(2)–Hf(1)–O(1)	71.1(3)
O(6)–Hf(1)–O(3)	93.7(4)	O(5)–Hf(1)–O(3)	165.8(4)
O(4)–Hf(1)–O(3)	75.7(4)	O(2)–Hf(1)–O(3)	70.8(3)
O(1)–Hf(1)–O(3)	70.5(3)	O(8)–Hf(2)–O(9)	98.9(5)
O(9)–Hf(2)–O(7)	103.5(5)	O(8)–Hf(2)–O(2)	102.8(4)
O(9)–Hf(2)–O(2)	102.7(5)	O(7)–Hf(2)–O(2)	139.8(3)
O(8)–Hf(2)–O(1)	165.3(4)	O(9)–Hf(2)–O(1)	95.7(4)
O(7)–Hf(2)–O(1)	75.6(4)	O(2)–Hf(2)–O(1)	71.9(3)
O(8)–Hf(2)–O(3)	94.6(4)	O(9)–Hf(2)–O(3)	166.2(4)
O(7)–Hf(2)–O(3)	75.7(4)	O(2)–Hf(2)–O(3)	71.7(3)
O(1)–Hf(2)–O(3)	70.7(3)	O(8)–Hf(2)–O(7)	102.7(5)
O(4)–Cu–O(7)	150.8(4)	O(4)–Cu–Cl	103.9(3)
O(7)–Cu–Cl	105.3(3)	O(4)–Cu–O(1)	79.0(4)
O(7)–Cu–O(1)	77.6(4)	Cl–Cu–O(1)	145.6(3)
O(4)–Cu–O(3)	78.2(4)	O(7)–Cu–O(3)	78.0(4)
Cl–Cu–O(3)	142.6(4)	O(1)–Cu–O(3)	71.8(3)
Hf(2)–O(1)–Hf(1)	95.0(3)	Hf(2)–O(2)–Hf(1)	97.8(3)
Hf(2)–O(3)–Hf(1)	94.1(3)	Cu–O(3)–Hf(2)	87.3(3)
Cu–O(3)–Hf(1)	86.4(3)	Hf(2)–O(3)–Hf(1)	94.1(3)
Cu–O(4)–Hf(1)	95.8(4)	Cu–O(7)–Hf(2)	96.2(4)

The constraints imposed in the formation of a chelating M_2X_9 bioctahedral sub-structure from an edge-sharing bioctahedron are evident in the distortion in geometries around two hafnium atoms [O(5)–Hf(1)–O(4) 106.6(4) and O(4)–Hf(1)–O(2) 139.6(4)°] when compared with the hafnium co-ordination in compound **1** (Table 1). The distorted trigonal-bipyramidal arrangement around Cu closely resembles the co-ordination sphere of Cd in $[CdM_2I(OPr^i)_9]$ derivatives. The trigonal plane of **5** is composed of the atoms Cu, Cl, O(3) and O(5) with two large and one very acute trigonal angle (Table 5). Among the equatorial ligands [Cl, O(3) and O(5)], chloride is most tightly bound to copper since the Cu–O distance [average 2.185(9) Å] is longer than the copper contact to the much larger chloride ion [2.144(5) Å]. However, the axial ligands [O(4) and O(7)] with bond lengths 2.001(10) and 2.008(10) Å are symmetrical. The metal–oxygen bond lengths in **5** follow the characteristic order (μ_3-OR > μ-OR > terminal OR) observed in the heterometal derivatives based on $M_2(OR)_9$ fragments and corroborate the lengthening of M–O bonds with increased bridging of alkoxide oxygen atoms.

Copper(II) being an odd-electron (d^9) system is prone to Jahn–Teller distortion which makes the co-ordination flexible and both normal co-ordinated (Cu–L) and longer semi-co-ordinated (Cu ··· L) bonds are possible.[21] In an attempt to define precisely the copper co-ordination in compound **5**, the copper–ligand distances and ligand–copper–ligand angles in a set of five-co-ordinated copper halide heterobimetallic derivatives $[CuM_2Cl(OPr^i)_9]$ (M = Ti **a**, Zr **b** or Hf **c**) are assembled in Table 6. Among five-co-ordinate copper complexes of type CuL_4L' (*cf.* CuO_4Cl in **a**–**c**) the observation of idealised square-pyrimidal (*SPY*) or trigonal-bipyramidal (*TBPY*) geometries is rather rare and often an intermediate arrangement is observed.[21]

The distorted-trigonal bipyramidal (*TBPY*) environment of copper in complexes **a**–**c** is most obvious in the bond angles in the equatorial plane which range from 70.8 to 145.9°, showing

L = O; L′ = Cl

significant deviation from ideal 120° angles. Also, the *trans* O–Cu–O angle (Table 6) in the three derivatives deviates (146.3–150.8°) from the ideal 180° value. However a tetrahedral distortion which will elongate the Cu–Cl bond is not conceivable, rather the larger chloride ion is found to be the most tightly bound ligand to copper and the average Cu–μ_3-O distances in these derivatives are longer (**b** and **c**) or comparable (**a**) to the Cu–Cl contacts (Table 6). In all the derivatives the longer distances from copper to triply bridged (μ_3) oxygens (sum of their ionic radii = 2.07 Å) are associated with highly acute trigonal O–Cu–O angles (Table 6) reflecting the distortion from a *TBPY* arrangement. Further, the Cu–μ_3-O distances, in **5**, are 0.16–0.18 Å longer than the symmetric Cu–μ-O distances whereas the difference between Hf–μ_3-O and Hf–μ-O distances is only 0.05 Å. In view of the observed bond anomalies, the copper co-ordination sphere in $[CuHf_2Cl(OPr^i)_9]$ can be termed as '3 + 2' with Cu–Cl, Cu–O(4) and Cu–O(7) being the stronger interactions and the co-ordination polyhedron of Cu^{2+} can be conceived as an intermediate conformation between an *elongated TBPY* and *compressed SPY* geometry.

$[\{[Cd(OPr^i)_3]Sr[Hf_2(OPr^i)_9]\}_2]$ 6. The formation of heterotermetallic frameworks $[\{[Cd(OPr^i)_3]Ba[M_2(OPr^i)_9\}_2]$ (M = Ti, Zr or Hf)[8a,12] from iodide heterobimetallic derivatives $[CdM_2I(OPr^i)_9]$ and $KBa(OPr^i)_3$ is accompanied by a switching of central metal atoms between precursor molecules and has been attributed to the larger size and pronounced tendency of Ba^{2+} to maximise its co-ordination number. A similar phenomenon has been observed in the isolation of **6** from $[CdHf_2I(OPr^i)_9]$ and $KSr(OPr^i)_3$. Although Sr^{2+} (1.18 Å) is significantly smaller than Ba^{2+} (1.35 Å) it is large enough (*cf.* Cd^{2+} 0.99 Å) to induce a rearrangement of metals required in the constitution of the heterotermetallic assembly $[\{[Cd(OPr^i)_3]Sr[Hf_2(OPr^i)_9]\}_2]$. This strategy of incorporating Sr^{2+} in molecular compounds has also been investigated with Ti and Zr as heterometal partners and the products obtained have been characterised by single-crystal X-ray crystallography.[22]

Compound **6** crystallises as a crystallographically imposed centrosymmetric dimer with a non-interacting benzene molecule in the crystal lattice. Selected bond lengths and angles are given in Table 7. The structural motif (Fig. 5) adopted is similar to the structures reported for barium derivatives. The overall molecule framework, when dissected formally, can be viewed as a $[Sr(\mu\text{-}OPr^i)_2Cd(\mu\text{-}OPr^i)_2Cd(\mu\text{-}OPr^i)_2Sr]^{2+}$ spirocyclic cationic unit which is capped at both the ends by sequestering confacial-bioctahedral $Hf_2(OPr^i)_9^-$ units. Alternatively in a triangular representation, which is obviously related to the barium derivatives, **6** can be viewed as a combination of two triangular $[SrHf_2(\mu_3\text{-}OPr^i)_2(\mu\text{-}OPr^i)_3(OPr^i)_4]^+$ units linked *via* a $[(Pr^iO)_2Cd(\mu\text{-}OPr^i)_2Cd(OPr^i)_2]^{2-}$ unit. Each hafnium and strontium atom is six-co-ordinate while cadmium has a distorted-tetrahedral arrangement of ligands. The Cd–O(12a) distance [2.152(9) Å] is much shorter than an average Cd–O dative bond[23] and is comparable with the Cd–O(12) bond length (2.17 Å), in agreement with the observed dimeric structure of **6** and symmetrical bridging in the four-membered $Cd(\mu\text{-}OPr^i)_2Cd$ unit. The Hf–O distances of the $Hf_2(OPr^i)_9$ unit in **6** vary in the following order: Hf–μ_3-O–Hf (average 2.234 Å) > Hf–μ-O–Hf (average 2.176 Å) > Hf–μ-O–Sr (average 2.033 Å) > Hf–O (terminal) (average 1.916 Å). The short Hf–O terminal bonds (Table 7) associated with obtuse Hf–O–C angles (average 170.67°) are typical of early transition-metal alkoxides. The co-ordination of strontium resembles a severely distorted octahedron with *cis* and *trans* angles ranging from 56.8 to 119.5 and 121.8(3) to

Table 6 Metrical comparison of copper–ligand bond distances and angles in a set of five-co-ordinate copper species $[CuM_2Cl(OPr^i)_9]$ (M = Ti **a**,[8b] Zr **b**[20] or Hf **c**)

	Bond length (Å)			Angles (°)	
	Axial	Equatorial			
Complex	Cu–O	Cu–Cl	Cu–O	Axial O–Cu–O	Trigonal
a	2.007, 2.008	2.172	2.157, 2.149	146.3	143.3, 145.9, 70.8
b	1.998, 1.999	2.164	2.207, 2.186	150.5	143.1, 145.6, 71.2
c	2.001, 2.008	2.144	2.183, 2.187	150.8	142.6, 145.6, 71.8

Table 7 Pertinent intratomic distance (Å) and angles (°) of compound **6**

Hf(1)–O(6)	1.918(10)	Hf(1)–O(7)	1.934(10)	Cd–O(12a)	2.152(9)	Cd–O(10)	2.170(8)
Hf(1)–O(3)	2.036(9)	Hf(1)–O(5)	2.165(10)	Cd–O(12)	2.171(9)	Cd–O(11)	2.172(9)
Hf(1)–O(2)	2.225(9)	Hf(1)–O(1)	2.249(8)	Sr–O(11)	2.406(9)	Sr–O(10)	2.428(9)
Hf(2)–O(9)	1.896(10)	Hf(2)–O(8)	1.917(11)	Sr–O(3)	2.571(9)	Sr–O(4)	2.610(10)
Hf(2)–O(4)	2.030(9)	Hf(2)–O(5)	2.187(10)	Sr–O(1)	2.642(8)	Sr–O(2)	2.650(8)
Hf(2)–O(1)	2.208(9)	Hf(2)–O(2)	2.254(8)	O(12)–Cd(a)	2.152(9)		
O(6)–Hf(1)–O(7)	99.5(6)	O(6)–Hf(1)–O(3)	99.8(5)	O(10)–Cd–O(12)	120.7(4)	O(12a)–Cd–O(11)	124.1(3)
O(7)–Hf(1)–O(3)	99.9(4)	O(6)–Hf(1)–O(5)	98.6(5)	O(10)–Cd–O(11)	85.9(3)	O(12)–Cd–O(11)	128.5(4)
O(7)–Hf(1)–O(5)	100.6(4)	O(3)–Hf(1)–O(5)	149.7(4)	O(11)–Sr–O(10)	75.5(3)	O(11)–Sr–O(3)	117.9(3)
O(6)–Hf(1)–O(2)	162.9(5)	O(7)–Hf(1)–O(2)	97.0(4)	O(10)–Sr–O(3)	104.1(3)	O(11)–Sr–O(4)	109.4(3)
O(3)–Hf(1)–O(2)	81.5(3)	O(5)–Hf(1)–O(2)	74.1(4)	O(10)–Sr–O(4)	119.5(3)	O(3)–Sr–O(4)	121.8(3)
O(6)–Hf(1)–O(1)	94.7(5)	O(7)–Hf(1)–O(1)	165.0(5)	O(11)–Sr–O(1)	172.6(3)	O(10)–Sr–O(1)	110.7(3)
O(3)–Hf(1)–O(1)	82.2(3)	O(5)–Hf(1)–O(1)	72.4(3)	O(3)–Sr–O(1)	65.5(3)	O(4)–Sr–O(1)	64.2(3)
O(2)–Hf(1)–O(1)	68.5(3)	O(9)–Hf(2)–O(8)	98.6(5)	O(11)–Sr–O(2)	117.7(3)	O(10)–Sr–O(2)	165.1(3)
O(9)–Hf(2)–O(4)	98.7(5)	O(8)–Hf(2)–O(4)	102.3(5)	O(3)–Sr–O(2)	64.5(3)	O(4)–Sr–O(2)	64.5(3)
O(9)–Hf(2)–O(5)	101.6(5)	O(8)–Hf(2)–O(5)	97.0(5)	O(1)–Sr–O(2)	56.8(2)	Hf(2)–O(1)–Hf(1)	94.1(3)
O(4)–Hf(2)–O(5)	149.5(4)	O(9)–Hf(2)–O(1)	97.0(4)	Hf(1)–O(1)–Sr	93.6(3)	Hf(2)–O(1)–Sr	95.1(3)
O(8)–Hf(2)–O(1)	162.9(4)	O(4)–Hf(2)–O(1)	82.2(4)	Hf(2)–O(2)–Sr	93.8(3)	Hf(1)–O(2)–Hf(2)	93.5(3)
O(5)–Hf(2)–O(1)	72.8(3)	O(9)–Hf(2)–O(2)	165.6(4)	Hf(2)–O(4)–Sr	100.7(4)	Hf(1)–O(2)–Sr	94.0(3)
O(8)–Hf(2)–O(2)	95.4(4)	O(4)–Hf(2)–O(2)	81.7(4)	Cd–O(10)–Sr	99.0(3)	Hf(1)–O(3)–Sr	101.2(3)
O(5)–Hf(2)–O(2)	73.0(3)	O(1)–Hf(2)–O(2)	68.7(3)	Cd(a)–O(12)–Cd	101.6(4)	Hf(1)–O(5)–Hf(2)	97.1(4)
O(12a)–Cd–O(10)	124.8(4)	O(12a)–Cd–O(12)	78.4(4)	Cd–O(11)–Sr	99.6(3)		

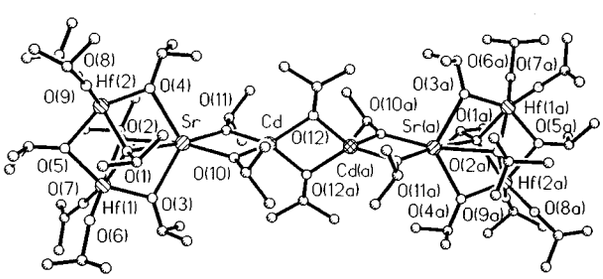

Fig. 5 Molecular structure of the centrosymmetric dimer $[\{[Cd(OPr^i)_3]Sr[Hf_2(OPr^i)_9]\}_2]$ **6** showing the atom labelling scheme used. Hydrogen atoms are not shown. Atoms designated with an 'a' are related by symmetry

172.6(3)°, respectively. The Sr atom shows different contacts to two doubly bridging oxygen atoms [Sr–O(3) 2.571(9), Sr–O(4) 2.610(10) Å] while the Sr–μ_3-O distances are comparable [2.642(8) and 2.650(8) Å].

Conclusion

We have used bioctahedral alkoxohafnate ligands $[Hf_2(OPr^i)_{10}]^{2-}$ and $[Hf_2(OPr^i)_9]^-$ with a variety of electrophiles (H^+, Li^+, Cu^{2+} and Sr^{2+}) to prepare hafnium-containing homo- and hetero-metallic alkoxides. Subject to the ligand–electrophile stoichiometry, both edge-sharing (**1**, **2** and **4**) and face-sharing (**5** and **6**) bioctahederal structures are observed. As a general feature, the present work demonstrates the preference of larger tetravalent early transition metals for six-co-ordination. Irrespective of the heterometal partner, hafnium atoms in all the structurally characterised derivatives are present in an octahedral geometry.

The tendency of Hf^{IV} to attain an octahedral surrounding of ligands is especially evident in the formation of compound **4** which in comparison to the titanium analogue $[\{LiTi(OPr^i)_5\}_2]$[20] (Li, four-co-ordination; Ti, five-co-ordination) shows a different co-ordination environment for the metals, in **4**, and a bond to Li (three-co-ordination) is sacrificed to satisfy the six-co-ordination of hafnium. This observation is strengthened in the easy formation and extraordinary stability of the bioctahedral $[Hf_2(OPr^i)_9]^-$ unit (**5** and **6**). This unit could be considered as a ligand-deficient derivative of $[Hf_2(OPr^i)_{10}]^{2-}$ [leaving one of the hafnium(IV) centres five-co-ordinate] where, despite the geometric constraints imposed in the transformation of an edge-sharing bioctahedron (**I**) to a confacial bioctahedron (**II**), the two metals form an additional isopropoxo bridge to achieve the six-co-ordination.

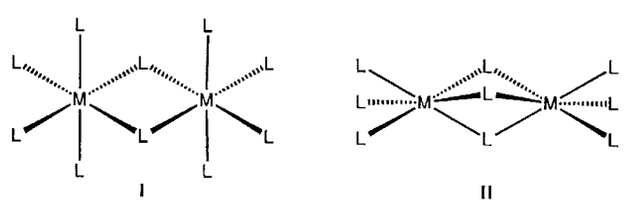

Experimental

Reagents and general techniques

All operations were carried out under a dry dinitrogen atmosphere with rigorous exclusion of oxygen and moisture. $[^2H_6]$-Benzene and $[^2H_8]$toluene were dried over molecular sieves and all other hydrocarbon solvents were distilled from lithium aluminium hydride and sodium–benzophenone. Isopropyl alcohol was dried by distillation from magnesium metal and aluminium

triisopropoxide. Pyridine was distilled from KOH and stored over 0.4 Å molecular sieves. Cryoscopy (C_6H_6, 5 °C) was used to estimate the nuclearity of the new compounds. Metal and halogen contents were determined using established analytical procedures.[24] The compound $[Sr(OPr^i)_2]_n$ was obtained by the alcoholysis of $[Sr\{N(SiMe_3)_2\}_2(thf)_2]$ (thf = tetrahydrofuran).[25] Copper(II) chloride and CdI_2 were dried by heating in vacuum and analysed for halogen contents before use. The NMR(^{1}H, ^{7}Li and ^{13}C) spectra were obtained on a Bruker AC-200 spectrometer, IR spectra on a Bio-Rad FTS-165 spectrometer. The ^{7}Li and ^{113}Cd NMR chemical shifts are referenced externally to 0.1 mol dm^{-3} solutions of LiCl and $Cd(NO_3)_2$ in D_2O, respectively. Analyses (C, H and N) were performed using a LECO Elemental Analyser CHN 900.

Preparations

$[Hf_2(OPr^i)_8(Pr^iOH)_2]$ 1. Hafnium isopropoxide **1** was synthesized following the literature method.[4] Elemental and spectral (IR and NMR) analyses, performed to check the identity of the product, conform to the reported values[6] and hence are not reproduced.

$[Hf_2(OPr^i)_8(Pr^iOH)(NC_5H_5)]$ 2. A crystalline sample of $[Hf_2(OPr^i)_8(Pr^iOH)_2]$ (2.45 g, 2.57 mmol) was heated *in vacuo* (150 °C, 10^{-2} Torr) for 30 min to obtain a viscous mass. The product was dissolved in toluene (10 cm^3) and pyridine (2 cm^3) was added. The solution was stirred for 1 h at 50 °C and left at room temperature overnight, when large rhombohedral crystals of compound **2** were formed. These were collected by decantation and dried in static vacuum. Yield: 1.35 g, 53% (Found: C, 39.5; H, 7.0; Hf, 35.95; N, 1.4. $C_{32}H_{68}Hf_2NO_9$ requires C, 39.7; H, 7.1; Hf, 36.9; N, 1.45%). NMR ($CDCl_3$, 20 °C): ^{1}H (200.13 MHz), δ 9.11 (br, 2 H, *o*-H of py), 7.32 (m, 2 H, *m*-H of py), 7.27 (t, 1 H, *p*-H of py), 4.44 (m, 9 H, CH) and 1.16 (d, 54 H, J = 6 Hz, CH_3); ^{13}C-{^{1}H} (50.3 MHz), δ 151.40, 137.93, 123.59 (*o*-, *p*-, *m*-C of py), 69.53 (CH) and 26.80 (CH_3). IR ($CDCl_3$, cm^{-1}): 3154 [br, ν(OH)], 1617m, 1479m, 1392s, 1330s, 1164s, 1027s, 848m, 813s, 774m and 665m. *M*: Found 1032; Calc. 968.

$[Hf_2(OPr^i)_8(Pr^iOH)(O_2C_4H_8)]$ 3. Compound **3** was synthesized in an analogous manner to that for **2** using $[Hf_2(OPr^i)_8(Pr^iOH)_2]$ (1.50 g, 1.57 mmol) and a toluene–1,4-dioxane mixture. Crystals were obtained from a concentrated solution at room temperature. Yield: 0.79 g, 51% (Found: C, 38.05; H, 7.2; Hf, 36.0. $C_{31}H_{70}Hf_2O_{11}$ requires C, 38.15; H, 7.25; Hf, 36.6%). NMR (C_6D_6, 20 °C): ^{1}H (200.13 MHz), δ 4.62 (m, 10 H, CH and OH), 3.67 (s, 8 H, CH_2) and 1.16 (d, 54 H, J = 6 Hz, CH_3); ^{13}C-{^{1}H} (50.3 MHz), δ 69.51 (CH), 67.87 (CH_2) and 26.34 (CH_3). IR ($CDCl_3$, cm^{-1}): 3154 [br, ν(OH)], 1617s, 1440s, 1372m, 1332m, 1253w, 1152s, 1012s, 980m, 774m and 610s. *M*: Found 1103; Calc. 976.

$[\{LiHf(OPr^i)_5\}_2]$ 4. To a toluene (10 cm^3) suspension of $LiOPr^i$ (0.41 g, 6.21 mmol) was added a clear solution of $[Hf_2(OPr^i)_8(Pr^iOH)_2]$ (2.94 g, 3.10 mmol) in hexane (20 cm^3) and the resulting mixture stirred at room temperature. The clear solution obtained was heated at 50 °C for ≈4 h and the volume reduced to ≈15 cm^3. The solution was cooled to −30 °C, producing colourless crystals overnight. A second crop was obtained by concentrating the mother-liquor. Yield: 1.01 g, 34% (Found: C, 37.0; H, 7.15; Hf, 36.9; Li, 1.4. $C_{30}H_{70}Hf_2Li_2O_{10}$ requires C, 37.5; H, 7.3; Hf, 37.1; Li, 1.45%). NMR ($C_6D_5CD_3$): ^{1}H (200.13 MHz, −10 °C), δ 4.71 (m, 3 H, J = 6, CH), 4.60 (spt, 2 H, J = 6, CH), 1.40 (d, 12 H, J = 6, CH_3), 1.38 (d, 12 H, J = 6) and 1.32 (d, 6 H, J = 6 Hz); ^{13}C-{^{1}H} (50.3 MHz, 20 °C), δ 69.95, 69.02, 67.68 (CH), 27.83, 27.66, 26.81 (CH_3); ^{7}Li (77.77 MHz, 20 °C), δ 3.02. *M*: Found 916; Calc. 962.

$[CuHf_2Cl(OPr^i)_9]$ 5. A benzene (20 cm^3) solution of freshly sublimed $[KHf_2(OPr^i)_9]$ (3.95 g, 4.26 mmol) was added to a benzene (15 cm^3) suspension of finely divided anhydrous $CuCl_2$ (0.58 g, 4.31 mmol) and the resulting mixture stirred at room temperature for ≈6 h. Over a few hours the solution gained a green coloration and an off-white precipitate remained. The mixture was heated at 70 °C for 3 h and the KCl formed was filtered off. All solvent was removed *in vacuo* to obtain a green solid. Dissolving the solid in the minimum volume of pentane followed by cooling at −10 °C gave green transparent crystals of compound **5**. Yield: 1.22 g, 29% (Found: C, 32.55; H, 6.2; Cl, 3.4; Hf, 35.85. $C_{27}H_{63}ClCuHf_2O_9$ requires C, 32.85; H, 6.4; Cl, 3.6; Hf, 36.15%). NMR ($C_6D_5CD_3$): ^{1}H (200.13 MHz, 20 °C), δ 4.27–4.70 (br, 9 H, CH), 1.44 (br, 6 H, CH_3), 1.35 (br, 12 H, CH_3) and 0.92 (br, 36 H, CH_3); (40 °C), δ 4.79 (br, 9 H, CH), 1.64 (br, ≈30 H, CH_3) and 1.24 (br, 24 H, CH_3); ^{13}C-{^{1}H} (50.3 MHz, 40 °C), δ 68.96, 67.54 (CH), 27.83, 27.40 (CH_3). *M*: Found 950; Calc. 988.

$[\{[Cd(OPr^i)_3]Sr[Hf_2(OPr^i)_9]\}_2]$ 6. (*a*) $[\{KSr(OPr^i)_3\}_n]$. Using freshly synthesized $Sr(OPr^i)_2$ and $KOPr^i$, $[\{KSr(OPr^i)_3\}_n]$ could be obtained by following the procedure described for $KBa(OPr^i)_3$[12] (Found: C, 35.15; H, 6.8; Sr, 29.0. $C_9H_{21}KO_3Sr$ requires C, 35.55; H, 6.95; Sr, 28.8%). NMR (C_6D_6, 20 °C): ^{1}H (200.13 MHz), δ 4.29 (m, 3 H, CH) and 1.35 (d, 18 H, CH_3); ^{13}C-{^{1}H} (50.3 MHz), δ 63.93 (CH) and 30.16 (CH_3). The poor solubility of the compound precluded molecular-weight studies.

(*b*) To a prestirred solution of $KSr(OPr^i)_3$ (0.35 g, 1.16 mmol) in benzene (10 cm^3) was added a solution of freshly sublimed $[CdHf_2I(OPr^i)_9]$ (1.31 g, 1.16 mmol) in benzene (15 cm^3) and the reaction mixture was stirred at room temperature for ≈12 h. After filtration of Kl and removal of volatiles, compound **6** was recovered as a white solid in almost quantitative yield (1.43 g, 97%). It was redissolved in a mixture of toluene–pentane and kept at 0 °C when colourless plates were formed. Yield: 0.82 g, 56% (Found: C, 35.45; H, 6.55; Cd, 8.55; Hf, 34.15; Sr, 6.8. $C_{78}H_{174}Cd_2Hf_4O_{24}Sr_2$ requires C, 35.9; H, 6.7; Cd, 8.6; Hf, 27.35; Sr, 6.7%). NMR (20 °C, $C_6D_5CD_3$): ^{1}H (200.13 MHz), δ 1.63 (d, 24 H, J = 6, CH_3), 1.51 (d, 36 H, J = 6, CH_3), 1.47 (d, 24 H, J = 6), 1.43 (d, 12 H, J = 6), 1.38 (d, 24 H, J = 6), 1.35 (d, 24 H, J = 6 Hz), CH protons observed as three overlapping septets centred at δ 4.64, 4.54 and 4.48; ^{13}C-{^{1}H} (50.3 MHz), δ 70.95, 69.53, 68.56, 67.94, 65.49 (CH), 30.47, 27.40, 26.77, 26.65, 26.49, 26.08 (CH_3); ^{113}Cd-{^{1}H} (44.3 MHz), δ 226.91. *M*: Found 2297; Calc. 2610.

X-Ray crystallography

Single crystals suitable for crystallography were selected from the bulk samples of compounds **1**, **2** and **4**–**6** and transferred in an inert atmosphere to Lindemann capillaries of appropriate dimensions. The sealed capillaries were then mounted on the goniometer head of a four-circle (Siemens AED for **4**–**6**) or an image-plate (Stoe IPDS for **1** and **2**) diffractometer operating with graphite-monochromated Mo-Kα radiation (λ = 0.710 73 Å) and the ω–θ scan technique (except in the case of **1** and **2**). In each case the cell constants and orientation matrix for data collection were obtained from a least-squares refinement using the setting angles of 25 reflections. Data collection for all the compounds was performed at 293(2) K. Lorentz-polarisation and absorption corrections (semiempirical from ψ scans for **4**–**6**, numerical for **1** and **2**) were applied to all the data. The structures were solved by a combination of direct methods (SHELXS 86)[26] and Fourier-difference techniques. The structures were refined (SHELXL 93)[27] by full-matrix least-squares analysis on F with anisotropic displacement parameters for all non-hydrogen atoms. All hydrogen atoms except that of OH in compounds **1** and **2** were idealised (C–H 0.96 Å) and included in the final stage of refinements with fixed isotropic parameters. Weights $\{w = q/[\sigma^2(F_o^2) + (aP)^2 + bP + d + e \sin\theta]$ where $P = [\max(0, F_o^2) + (1 - f)F_c^2]\}$ were included in the last refinement cycles.

Table 8 Summary of crystallographic data for compounds **1**, **2** and **4**–**6**

	1	**2**	**4**	**5**	**6**
Empirical formula	$C_{30}H_{70}Hf_2O_{10}$	$C_{32}H_{68}Hf_2NO_9$	$C_{30}H_{70}Hf_2Li_2O_{10}$	$C_{27}H_{63}ClCuHf_2O_9$	$C_{78}H_{174}Cd_2Hf_4O_{24}Sr_2$
M	947.84	967.85	961.72	987.74	2610.17
Crystal system	Triclinic	Monoclinic	Triclinic	Monoclinic	Monoclinic
Space group	$P\bar{1}$	$C2/c$	$P\bar{1}$	$P2_1/n$	$P2_1/c$
a/Å	12.118(2)	10.501(2)	9.963(2)	9.778(2)	22.800(5)
b/Å	12.212(2)	18.076(4)	10.895(2)	24.360(5)	12.894(3)
c/Å	14.964(3)	22.859(5)	12.123(2)	16.826(3)	19.260(4)
α/°	80.69(3)		66.65(3)		
β/°	84.91(3)	90.94(3)	68.21(3)	93.06(3)	96.20(3)
γ/°	88.89(3)		70.04(3)		
U/Å^3	2176.6(7)	4338(2)	1092.3(3)	4002.1(14)	5629(2)
Z	2	4	1	4	2
F(000)	948	1932	480	1948	2588
D_c/g cm^{-3}	1.446	1.482	1.462	1.639	1.540
Crystal size/mm	0.5 × 0.4 × 0.2	0.3 × 0.2 × 0.15	0.4 × 0.3 × 0.25	0.45 × 0.33 × 0.3	0.5 × 0.3 × 0.15
Standard reflections	50–250	50–200	3	3	3
θ Range/°	2.54–26.13	2.25–24.13	1.90–22.49	1.67–24.99	1.80–22.50
Reflections collected	21 630	10 197	2857	7261	8062
Independent reflections	8013	3408	2857	7040	7346
Observed reflections [$I > 2\sigma(I)$]	6182	3016	2711	5586	5859
Goodness of fit on F^2	1.089	1.053	1.187	1.151	1.049
Final R indices [$I > 2\sigma(I)$]	0.0655	0.0544	$R1 = 0.0456$	$R1 = 0.0725$	0.0694
(all data)	0.0796	0.0594	$R1 = 0.0486$	$R1 = 0.0940$	0.0884
Largest difference peak and hole/e Å^{-3}	1.295, −2.545	1.602, −1.157	1.235, −1.576	1.236, −1.657	0.889, −1.439

Atomic coordinates, thermal parameters, and bond lengths and angles have been deposited at the Cambridge Crystallographic Data Centre (CCDC). See Instructions for Authors, *J. Chem. Soc.*, *Dalton Trans.*, 1997, Issue 1. Any request to the CCDC for this material should quote the full literature citation and the reference number 186/503.

Acknowledgements

We gratefully acknowledge the generous support of Deutsche Forschungsgemeinschaft under the framework of the programme SFB-277 and the Alexander von Humboldt Foundation, Germany for a research fellowship (to S. M.).

References

1 G. J. Ashwell (Editor), *Molecular Electronics*, Wiley, New York, 1992.
2 R. C. Mehrotra, A. Singh and S. Sogani, *Chem. Rev.*, 1994, **94**, 1643; K. G. Caulton and L. G. Hubert-Pfalzgraf, *Chem. Rev.*, 1990, **90**, 969.
3 W. S. Rees, jun. (Editor), *CVD of Non-metals*, VCH, Weinheim, 1996.
4 D. C. Bradley, R. C. Mehrotra and D. P. Gaur, *Metal Akoxides*, Academic Press, London, 1978.
5 M. J. Hampden-Smith, T. A. Wark, A. Rheingold and J. C. Huffman, *Can. J. Chem.*, 1991, **69**, 121.
6 B. A. Vaartstra, J. C. Huffman, P. S. Gradeff, L. G. Hubert-Pfalzgraf, J. C. Daran, S. Parrand, K. Yunulu and K. G. Caulton, *Inorg. Chem.*, 1990, **29**, 3126.
7 C. Favotto, A. Margaillan and M. Roubin, *Ann. Chim.* (*Paris*), 1996, **21**, 13.
8 M. Veith, S. Mathur and V. Huch, *Inorg. Chem.*, (*a*) 1996, **35**, 7295; (*b*) in the press.
9 H. Nagamoto, K. Amanuma, H. Nobutomo and H. Inoue, *Chem. Lett*, 1988, **2**, 237.
10 H. Maeda, Y. Tanaka, M. Fukutomi and T. Asane, *Jpn. J. Appl. Phys.*, 1988, **27**, L209.
11 P. Pereira, S. H. Lee, G. A. Somaraji and H. Heinemann, *Catal. Lett.*, 1990, **6**, 255.
12 M. Veith, S. Mathur and V. Huch, *J. Am. Chem. Soc.*, 1996, **118**, 903.
13 R. J. Cava, R. B. van Dover, B. Batlagg and E. A. Rietman, *Phys. Rev. Lett.*, 1987, **58**, 408.
14 (*a*) A. A. Pinkerton, D. Schwarzenbach, L. G. Hubert-Pfalzgraf and J. G. Riess, *Inorg. Chem.*, 1976, **15**, 1196; (*b*) E. P. Turevskaya, N. Ya. Turova, A. V. Korolev, A. I. Yanovsky and Yu. T. Struchkov, *Polyhedron*, 1995, **14**, 1531.
15 M. Chisholm and D. L. Clark, *Comments Inorg. Chem.*, 1987, **6**, 23.
16 C. K. Johnson, ORTEP, Report ORNL-5138, Oak Ridge National Laboratory, Oak Ridge, TN, 1976.
17 M. Veith, *Chem. Rev.*, 1990, **90**, 3.
18 M. J. Hampden-Smith, D. S. Williams and A. L. Rheingold, *Inorg. Chem.*, 1990, **29**, 4076.
19 M. Veith, S. Mathur and V. Huch, *J. Chem. Soc., Dalton Trans.*, 1996, 2485.
20 B. A. Vaartstra, J. A. Samuels, E. H. Barash, J. D. Martin, W. E. Streib, C. Gasser and K. G. Caulton, *J. Organomet. Chem.*, 1993, **449**, 191.
21 D. Reinen and C. Friebel, *Inorg. Chem.*, 1984, **23**, 791; J. D. Blanchette and R. D. Willett, *Inorg. Chem.*, 1988, **27**, 843.
22 M. Veith and S. Mathur, unpublished work.
23 S. C. Goel, M. Y. Chiang and W. E. Buhro, *J. Am. Chem. Soc.*, 1991, **112**, 6724.
24 A. I. Vogel, *A Textbook of Quantitative Inorganic Analysis*, Longmans, London, 1978.
25 M. Westerhausen, *Inorg. Chem.*, 1991, **30**, 96.
26 G. M. Sheldrick, SHELXS 86, Program for Crystal Structure Determination, University of Göttingen, 1986.
27 G. M. Sheldrick, SHELXS 93, Program for Crystal Structure Determination, University of Göttingen, 1993.

Received 5*th February* 1997; *Paper* 7/00833C